Institute of Physics Publishing Journal of Physics: Conference Series **38** (2006) 120–125
doi:10.1088/1742-6596/38/1/030 NPMS-7/SIMD-5 (Maui 2005)

Transport Properties of Beam-Deposited Pt Nanowires

F. Wakaya*, Y. Tsukatani, N. Yamasaki, K. Murakami, S. Abo and M. Takai

KYOKUGEN Research Center, Osaka University, 1-3 Machikaneyama, Toyonaka, Osaka 560-8531, Japan

*Email: wakaya@rcem.osaka-u.ac.jp

Abstract.
Pt wires were fabricated by using electron-beam (EB) and Ga focused-ion-beam (FIB) irradiation while providing $C_5H_5Pt(CH_3)_3$ gas through a nozzle. Electron transport properties of the wires were investigated. The resistance of the EB-deposited wires was quite high as deposited but was reduced by 3–4 orders of magnitude after 400–500°C annealing. The electron transport of the as-deposited EB-deposited wire was dominated by the variable range hopping and the Coulomb blockade simultaneously, and showed the antilocalization effect after 400°C annealing. The electron phase-breaking length in the EB-deposited wire with 400°C annealing, which was derived from a theoretical fitting, is ≈10 nm at ≈4 K and increases with decreasing temperature. This means that 10-nm fabrication technology and improvement of coherence length are required for coherent vacuum nanoelectronics.

1. Introduction

Vacuum nanoelectronics is one of the promising fields for future electronics. Using electrons in nano vacuum tubes enables us to realize very fast switching devices, robust devices against cosmic rays, flat panel displays, etc. We have succeeded in fabricating field-emission electron sources using Pt tips deposited by electron-beam (EB) irradiation and characterized the emission properties[1–3]. The technique of EB and focused-ion-beam (FIB) induced deposition is thus a powerful tool for fabricating various nanostructures at arbitrary positions on a substrate.

The interference effects of electrons emitted from two emission sites on an emitter fabricated by beam-induced deposition are being studied very recently[4]. Such interference effects may open a new field of *coherent vacuum nanoelectronics*. An electron can pass through the two emission sites while maintaining the coherence as in Young's experiment in optics if the two emission sites are located within the coherence length of the emitter material. There are some reports[5,6] which describe that electrons emitted from the neighboring pentagons of a carbon nanotube (CNT) show interference effects. This should be due to the fact that the pentagons on top of the CNT are located within the electron coherence length in the CNT. The emission sites on the coherent electron emitter should, thus, be located within the coherence length to observe the interference effects. It is, therefore, important to investigate electron transport properties and coherent electron character of nanostructures fabricated by the beam-induced deposition.

This paper describes fabrication and characterization of Pt wires and presents a discussion of the transport properties of the Pt wires formed by EB- and FIB-induced deposition.

© 2006 IOP Publishing Ltd

Report Documentation Page

Form Approved
OMB No. 0704-0188

Public reporting burden for the collection of information is estimated to average 1 hour per response, including the time for reviewing instructions, searching existing data sources, gathering and maintaining the data needed, and completing and reviewing the collection of information. Send comments regarding this burden estimate or any other aspect of this collection of information, including suggestions for reducing this burden, to Washington Headquarters Services, Directorate for Information Operations and Reports, 1215 Jefferson Davis Highway, Suite 1204, Arlington VA 22202-4302. Respondents should be aware that notwithstanding any other provision of law, no person shall be subject to a penalty for failing to comply with a collection of information if it does not display a currently valid OMB control number.

1. REPORT DATE	2. REPORT TYPE	3. DATES COVERED
2006	**N/A**	**-**

4. TITLE AND SUBTITLE	5a. CONTRACT NUMBER
Transport Properties of Beam-Deposited Pt Nanowires	5b. GRANT NUMBER
	5c. PROGRAM ELEMENT NUMBER
6. AUTHOR(S)	5d. PROJECT NUMBER
	5e. TASK NUMBER
	5f. WORK UNIT NUMBER
7. PERFORMING ORGANIZATION NAME(S) AND ADDRESS(ES) **KYOKUGEN Research Center, Osaka University, 1-3 Machikaneyama, Toyonaka, Osaka 560-8531, Japan**	8. PERFORMING ORGANIZATION REPORT NUMBER
9. SPONSORING/MONITORING AGENCY NAME(S) AND ADDRESS(ES)	10. SPONSOR/MONITOR'S ACRONYM(S)
	11. SPONSOR/MONITOR'S REPORT NUMBER(S)

12. DISTRIBUTION/AVAILABILITY STATEMENT
Approved for public release, distribution unlimited

13. SUPPLEMENTARY NOTES
The Seventh International Conference on New Phenomena in Mesoscopic Structures & The Fifth International Conference on Surfaces and Interfaces of Mesoscopic Devices, November 27th - December 2nd, 2005, Maui, Hawaii, USA

14. ABSTRACT

15. SUBJECT TERMS

16. SECURITY CLASSIFICATION OF:			17. LIMITATION OF ABSTRACT	18. NUMBER OF PAGES	19a. NAME OF RESPONSIBLE PERSON
a. REPORT	b. ABSTRACT	c. THIS PAGE			
unclassified	**unclassified**	**unclassified**	**SAR**	**6**	

2. Experimental

The starting material was a Si wafer whose surface was thermally oxidized. Electron-beam lithography, sputter deposition of Au/Ti, and lift-off technique were used to fabricate registration marks and electrodes. Pt nanowires were deposited by 15-keV EB or 30-keV Ga FIB irradiation with $C_5H_5Pt(CH_3)_3$ gas provided through a nozzle. The base pressure of the beam-induced-deposition system was 10^{-6} – 10^{-7} mbar. The height (h) of the fabricated Pt wire was measured using an atomic force microscope, while the width (W) and the length (L) were measured by scanning-electron-microscope (SEM) observation. SEM micrographs of typical specimens, which were fabricated using Ga FIB, are shown in Fig. 1.

Electron transport characteristics were measured using a cryo system between 4–300 K. A dilution refrigerator was also used for measuring at temperatures down to 100 mK. The magnetoresistance was measured in a magnetic field perpendicular to the substrate.

3. Results and discussion

The resistivity of the EB-deposited Pt, which was obtained from the measured zero-bias resistance and the sample dimension, was quite high (≈ 1 Ωcm) as deposited and became much higher with decreasing temperature, while the resistivity of the FIB-deposited Pt wires was low (≈ 10^{-3} Ωcm) and hardly depended on temperature. Figure 2(a) shows the resistance of the EB-deposited Pt wire, which was in two-terminal configuration with gate electrodes as shown in Fig. 1(a), as a function of temperature. The observed temperature T dependence of the resistance $R \propto \exp(T_0/T)^{1/2}$, where T_0 is a constant, means that the electron conduction was dominated by the variable range hopping (VRH)[7,8].

Figure 2(b) shows the measured gate-voltage dependence of the current at several temperatures, where the gate voltage was applied at the two in-plane side gates. The *periodic* Coulomb oscillations were observed at temperatures up to ≈200 K, which means that a *single* Coulomb island dominated the Coulomb blockade characteristics. We observed leakage current in the Coulomb gap, partially due to the high temperature, resulting in that clear Coulomb gap modulation (Coulomb diamond) was not observed.

As shown in Figs. 2(a) and (b), the electron transport of the EB-deposited Pt wires was dominated by the VRH and the Coulomb blockade simultaneously. The hopping transport with Coulomb interaction is quite interesting transport regeme[9,10]. The observed temperature dependence of the resistance $R \propto \exp(T_0/T)^{1/2}$ might be that predicted in the case of VRH with Coulomb interaction[9]. The authors of refs. 11 and 12 reported that the Pt nanocrystals are distributed in the amorphous carbon matrix in the wire deposited by EB irradiation with $C_5H_5Pt(CH_3)_3$ gas. Although the detailed mechanisms for the observed VRH and the Coulomb oscillation are unclear, the possible candidates for the small conductive sites in VRH conduction and for the Coulomb island are the Pt nanocrystals or isolated electron sites in the amorphous carbon.

As described above, the EB-deposited wires showed quite high resistance, which might cause problems when they were used for the electron emitter. In order to reduce the resistance the annealing effects were investigated using four different samples and are summarized in Fig. 3(a), where the samples were in the 4-terminal configuration as shown in Fig. 1(b) with the separation between electrodes were 1 μm. The resistance of all samples investigated reduced from ≈10^6 Ω as deposited to ≈500 Ω after 400–500°C annealing. Although the EB-deposited wires were almost insulators at low temperatures like 4.2 K as deposited, they showed metallic conduction after annealing. The temperature dependence of the resistivity of the EB-deposited wires after annealing is similar to that of the FIB-deposited wires without annealing, as discussed elsewhere[13]. The magnetoresistance of the EB-deposited wires annealed at 400°C was measured from 100 mK – 4.2 K using two-terminal configuration. The fit of the measured positive magnetoresistances with the theoretical expression provides the phase-breaking length l_ϕ, which is summarized in Fig. 3(b) for two different samples as a function of temperature. The obtained l_ϕ is ≈10 nm at ≈4 K, which is similar to that for the FIB-

deposited wire[13]. l_ϕ increases with decreasing temperature and seems to saturate as is often observed in disordered metals[14]. The dashed line in Fig. 3(b) indicates the $T^{-1/3}$ slope, which is predicted where l_ϕ is dominated by the Nyquist dephasing mechanism in one dimension. Except for the saturation at low temperature, the slope of experimentally obtained l_ϕ was steeper than the $T^{-1/3}$ slope. This deviation might be due to the other dephasing mechanisms.

The authors in refs. 11 and 14 reported on the transport properties of Pt nanowires fabricated by EB[11] and FIB[14] irradiation with the same precursor gas as this work. Although the fabrication processes are quite similar, the transport properties are different. The l_ϕ reported by them is larger than that in the present work and in ref. 13. This means that longer l_ϕ, which is important for the coherent electron emitters, may be realized by optimization of the process and structural parameters.

4. Summary

The EB- and FIB-induced deposition technique with $C_5H_5Pt(CH_3)_3$ gas was utilized to fabricate Pt wires. The EB-deposited wires showed quite high resistance as deposited. Electron transport in the EB-deposited wires was dominated simultaneously by VRH and the Coulomb blockade. The room-temperature resistance of the EB-deposited wire after 400–500°C annealing decreased by 3–4 orders of magnitude. The EB-deposited wire after 400 °C annealing showed metallic conduction and coherent transport properties, i.e., the antilocalization effect, at low temperature. The observed magnetoresistance with theoretical fitting provides the phase-breaking length of electrons in the wire, which is ≈10 nm at ≈4 K. This means that 10-nm fabrication technology and improvement of coherence length are required for the coherent vacuum nanoelectronics. Furthermore, nanofabrication technology less than 10 nm should be the key technology for room-temperature operation of coherent-vacuum-nanoelectronic devices.

References

[1] Jarupoonphol W, Ochiai C, Takai M, Hosono A and Okuda S 2002 Jpn. J. Appl. Phys. **41** 4311
[2] Murakami K, Jarupoonphol W, Sakata K, Takai M 2003 Jpn. J. Appl. Phys. **42** 4037
[3] Murakami K, Yamasaki N, Abo S, Wakaya F and Takai M 2005 J. Vac. Sci & Technol. B **23** 759
[4] Murakami K, Yamasaki N, Abo S, Wakaya F and Takai M 2005 J. Vac. Sci & Technol. B **23** 735
[5] Saito Y, Hata K and Murata T 2000 Jpn. J. Appl. Phys. **39** L271
[6] Oshima C, Matsuda K, Kona T, Mogami Y, Yamashita T, Saito Y, Hata K and Takakura A 2003 J. Vac. Sci & Technol. B **21** 1700
[7] Koops H W P, Schrössler C, Kaya A and Weber M 1996 J. Vac. Sci. & Technol. B **14** 4105
[8] Mott N F 1987 *Conduction in Non-Crystalline Materials* (Oxford University Press, Oxford)
[9] Efros A L and Shklovskii B I 1975 J. Phys. C: Solid State Phys. **8** L49
[10] Fransson J, Lin J –F, Rotkina L, Bird J P, Bennett P A 2005 Phys. Rev. B **72** 113411
[11] Rotkina L, Lin J -F and Bird J P 2003 Appl. Phys. Lett. **83** 4426
[12] Koops H W P, Kaya A and Weber M 1995 J. Vac. Sci. &I Technol. B **13** 2400
[13] Tsukatani Y, Yamasaki N, Murakami K, Wakaya F and Takai M 2005 Jpn. J. Appl. Phys. **44** 5683
[14] Lin J -F, Bird J P, Rotkina L and Bennett P A 2003 Appl. Phys. Lett. **82** 802

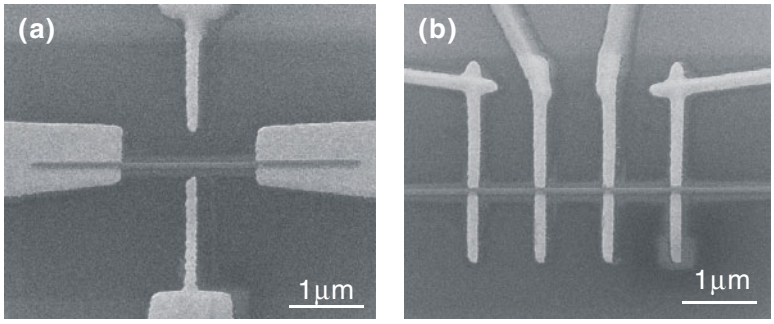

Fig. 1: SEM micrographs of typical specimens for (a) two-terminal configuration with gate electrodes and (b) four-terminal configuration. The bright regions are the Au/Ti electrodes on the SiO_2/Si surface. The horizontal thin lines in the middle are the FIB-deposited Pt wire.

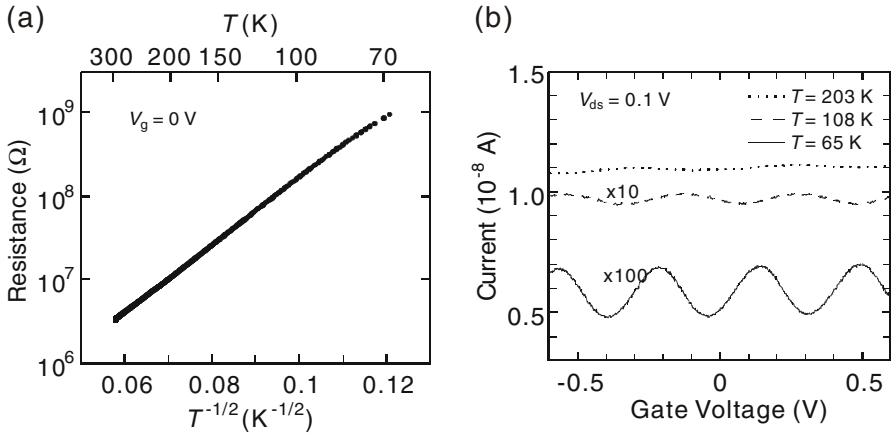

Fig. 2: (a) Temperature dependence of zero-bias resistance of the EB-deposited wire (L = 2 μm, W = 350 nm, h = 100 nm). The dependence of $R \propto \exp(T_0 / T)^{1/2}$ is due to the VRH. (b) Gate-voltage dependence of the current (same sample as (a)). Periodic Coulomb oscillations were observed.

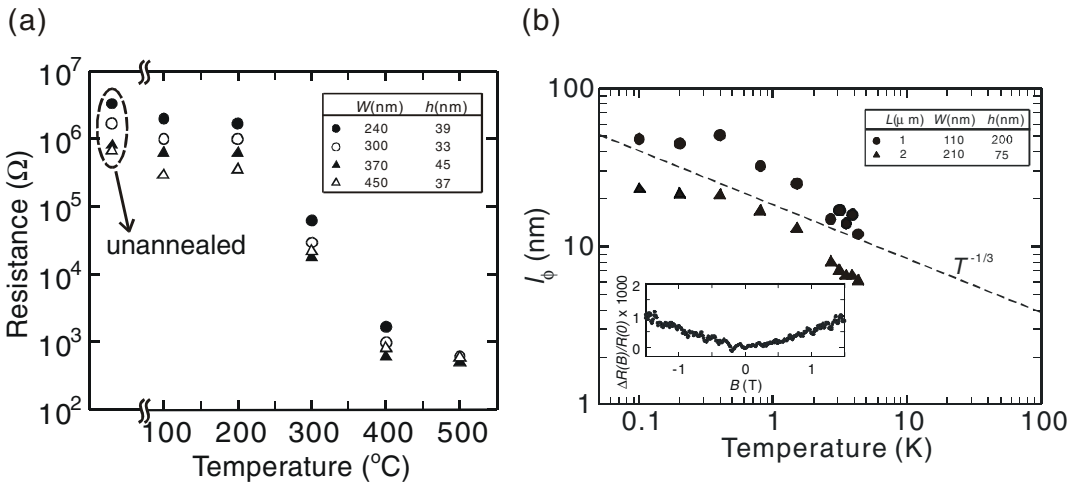

Fig. 3: (a) Room-temperature resistance of EB-deposited wires as a function of annealing temperature. Four different samples were measured, whose dimensions are summarized in the figure. (b) Temperature dependence of l_ϕ in EB-deposited wires. The dashed line indicates the $T^{-1/3}$ slope, which predicted for the Nyquist dephasing mechanism in one dimension. The lower inset shows the magnetoresistance of the 1-μm sample at 2.7 K.